Advances in Computational Design, *Vol. 10, No. 2 (2025) 127-149*
https://doi.org/10.12989/acd.2025.10.2.127

Using the cheetah optimizer for cost reduction in shell-and-tube and plate-fin heat exchangers

Makadia Jiten Jayantilal* and Maniar Nirav Pravinchandra[a]

Mechanical Engineering Department, *VVP Engineering College*, *Rajkot*, *Gujarat*, *India*

(Received January 2, 2025, Revised March 17, 2025, Accepted April 1, 2025)

Abstract. This study investigates the effectiveness of the Cheetah Optimizer for optimizing heat exchanger designs, specifically for shell and tube and plate fin heat exchangers. The optimizer's performance was validated through comparisons with established metaheuristic methods, ensuring robust results. In the case of shell and tube heat exchangers, the Cheetah Optimizer achieved a 3% reduction in overall costs compared to Particle Swarm Optimization (PSO). While the Cheetah Optimizer did not outperform α-EHO and Gravitational Search Algorithm (GSA) in the first case study, it surpassed both in the second case. For plate fin heat exchangers, the Cheetah Optimizer demonstrated superior performance over the Imperialist Competitive Algorithm and Teaching Learning-Based Optimization. These findings confirm the Cheetah Optimizer as a viable and competitive alternative for heat exchanger design optimization, particularly in certain scenarios.

Keywords: cheetah optimizer; computational geometry; design optimization; heat exchanger

1. Introduction

The design and optimization of heat exchangers have been critical to a wide range of industries, with particular focus on improving performance, efficiency, and cost-effectiveness. Over the years, various methodologies and techniques have been developed to enhance heat exchanger design, from the traditional methods to modern, computationally advanced optimization algorithms. This literature review summarizes key studies and milestones in heat exchanger design, focusing on the evolution of methodologies and optimization techniques. The foundation of heat exchanger design is rooted in classical heat transfer theory, as laid out in seminal works such as Kern's Process Heat Transfer (1950), which remains a core reference for understanding the principles of heat transfer in various processes. Building on this, Coulson and Richardson (1996) provided an extensive overview in Chemical Engineering, presenting key insights into the fundamentals of heat transfer and fluid flow in chemical engineering applications, including heat exchangers. In the mid-1990s, heat exchanger design expanded further with works like those of Manglik and Bergles (1995), who developed heat transfer and pressure drop correlations for offset strip fin compact heat exchangers. The work represented a significant leap in compact heat exchanger technology, with broad

*Corresponding author, Assistant Professor, E-mail: jitenpateler@gmail.com
[a] Professor, E-mail: maniarniravp@gmail.com

 ISSN: 2383-8477 (Print), 2466-0523 (Online)

implications for improving thermal performance and space efficiency. Incropera *et al*. (1996) in Fundamentals of Heat and Mass Transfer provided a comprehensive textbook that underpinned much of the research in heat exchanger design, integrating heat transfer, thermodynamics, and fluid mechanics into a unified approach. This laid the groundwork for the later development of computational methods and design optimizations.

As the field progressed into the 2000s, there was a significant push towards applying more sophisticated mathematical modelling and optimization techniques. Shah and Sekulic (2003) introduced their work on the Fundamentals of Heat Exchanger Design, which helped bridge the gap between theoretical heat transfer concepts and practical design applications. Insights provided the foundation for modern heat exchanger design tools. Mizutani *et al*. (2003) explored the integration of heat-exchanger network synthesis with detailed heat exchanger designs using mathematical programming. This interdisciplinary approach opened up new avenues for optimizing heat exchanger systems within industrial networks. Furthermore, Taal *et al*. (2003) delved into the economic evaluations of retrofit projects, offering insights into cost estimation and energy price forecasts, critical for making economically viable decisions in heat exchanger design.

By the late 2000s, the focus shifted towards optimizing heat exchangers using advanced computational methods. Studies by Serna-González *et al*. (2007) provided insight into the feasible design space for shell-and-tube heat exchangers, demonstrating the effectiveness of optimization methods like the Bell-Delaware method. Similarly, Babu and Shaik (2007) employed differential evolution strategies for optimal shell-and-tube heat exchanger design, highlighting the importance of evolutionary algorithms in improving heat exchanger performance. Xie *et al*. (2008) and Caputo *et al*. (2008) expanded the understanding of heat exchanger optimization by applying genetic algorithms and economic optimization methods. These studies focused on fin-and-tube and shell-and-tube designs, respectively, and emphasized the need for balancing multiple objectives in heat exchanger design, such as heat transfer, pressure drop, and cost. The application of metaheuristic algorithms to heat exchanger design became more prominent in the 2010s. Fesanghary *et al*. (2009) utilized global sensitivity analysis and the harmony search algorithm for design optimization, while Silva *et al*. (2010) and Patel and Rao (2010) explored particle swarm optimization (PSO) as an effective tool for optimizing heat exchangers. These studies demonstrated the growing reliance on computational intelligence techniques to solve complex design problems. Yousefi *et al*. (2012) introduced the imperialist competitive algorithm for plate-fin heat exchangers, further solidifying the role of evolutionary algorithms in heat exchanger optimization. In the following years, Ghanei *et al*. (2014) and Thuy *et al*. (2014) built upon these foundations by applying PSO for multi-objective optimization of shell-and-tube heat exchangers, considering both thermal and economic aspects of design. By the mid-2010s, the focus shifted towards more sophisticated optimization methods. Yousefi *et al*. (2015) implemented multi-stage thermal-economic optimization for compact heat exchangers, showcasing the importance of evolutionary algorithms in real-world applications. Kaveh and Farhoudi (2016) introduced dolphin echolocation optimization, and later Kaveh and Rezaei (2016) employed ECBO for dome structures, signalling the increased use of novel optimization algorithms in engineering design. In the following years, Mekki *et al*. (2021) utilized genetic algorithm-based topology optimization for heat exchanger fins in aerospace applications, highlighting the growing significance of aerospace-related heat exchanger optimization. Similarly, Hajabdollahi *et al*. (2021) explored optimization algorithms across different types of heat exchangers, showing the diversity of applications in modern heat exchanger design. The latest studies, including those by Saldanha *et al*. (2021), Bahiraei *et al*. (2021), and Makadia (2021), continue to refine optimization techniques by

combining neural networks with nature-inspired algorithms and evolutionary computation. These advancements illustrate the integration of machine learning and AI with traditional optimization methods to enhance the design process. New optimization algorithms, such as the cheetah optimizer proposed by Akbari *et al*. (2022), and recent metaheuristic approaches like those presented by Jafari-Asl *et al*. (2024) for reliability-based design, signal a continuing trend towards more intelligent and efficient design methodologies. Furthermore, Mohapatra *et al*. (2024) introduced a novel opposition-based orthogonal learning method for plate-fin heat exchangers, emphasizing the increasing sophistication of optimization techniques. Montano *et al* (2025) recently proposed new algorithm named success-based optimization (SBO), however, it is only tested on mathematical benchmark function, henceforth, its real-world application is not yet proved. The evolution of heat exchanger design has been marked by the steady incorporation of advanced optimization techniques, from early mathematical models to modern metaheuristic and AI-driven algorithms. As research progresses, optimization algorithms such as genetic algorithms, particle swarm optimization, and newer methods like the cheetah optimizer are driving innovations in heat exchanger design, promising more efficient, cost-effective, and reliable solutions for industrial applications.

2. Cheetah optimizer

Akbari *et al*. (2022) proposed the Cheetah optimizer as an advanced algorithm designed for efficient and rapid optimization tasks, particularly in machine learning and deep learning contexts. The algorithm focuses on accelerating convergence rates while maintaining high accuracy in various optimization problems. By utilizing adaptive learning rates and momentum techniques, Cheetah effectively navigates the search space, making the algorithm suitable for handling complex functions and large datasets. Key features of the Cheetah optimizer include the ability to dynamically adjust parameters based on the landscape of the loss function, which enhances performance on non-convex optimization tasks. The implementation is often praised for being lightweight and easy to integrate into existing frameworks, allowing for seamless adaptation in various applications. Overall, the Cheetah optimizer stands out for its balance between speed and reliability, making the algorithm a popular choice among researchers and practitioners looking to optimize models efficiently. The algorithm pseudo code is presented below.

These novel aspects make the Cheetah Optimizer a promising tool for the evolving field of heat exchanger optimization, particularly where traditional methods may fall short in terms of efficiency, cost, and convergence speed.

Adaptation of a New Optimization Algorithm: The Cheetah Optimizer, an advanced metaheuristic algorithm, introduces a fresh approach to solving complex optimization problems. Unlike traditional methods, such as Particle Swarm Optimization (PSO) or Genetic Algorithms (GA), the Cheetah Optimizer focuses on accelerating convergence while maintaining high accuracy, offering an efficient alternative for optimization tasks in heat exchanger design.

Efficient Search Space Navigation: The Cheetah Optimizer's ability to dynamically adjust parameters based on the landscape of the loss function enhances performance, especially for non-convex optimization tasks common in heat exchanger design. This feature makes it particularly well-suited for handling the intricate and multi-objective nature of heat exchanger optimization.

Performance in Complex Design Scenarios: By outperforming established methods like PSO, Imperialist Competitive Algorithm (ICA), and Teaching Learning-Based Optimization (TLBO) in

certain heat exchanger design problems, the Cheetah Optimizer demonstrates a competitive edge in terms of speed, cost reduction, and overall optimization quality.

Cost Reduction and Efficiency: The Cheetah Optimizer achieves notable cost reductions (e.g., a 3% reduction in shell and tube heat exchanger optimization), highlighting its potential to drive cost-effective design solutions in industrial applications.

Flexibility and Robustness: The Cheetah Optimizer has shown robust performance in various case studies, handling both shell-and-tube and plate-fin heat exchangers. This versatility suggests that the algorithm can be adapted for a wide range of heat exchanger design scenarios, offering broader application potential in thermal systems optimization.

```
function best_solution = cheetah_optimizer()
    % Step 1: Initialize Parameters
    population_size = 100; % Example value
    max_iterations = 1000; % Example value
    dimension = 10; % Number of variables in the solution
    lower_bound = -10; % Lower bound of the search space
    upper_bound = 10; % Upper bound of the search space

    % Step 2: Initialize Population
    cheetahs = initialize_population(population_size, dimension, lower_bound, upper_bound);

    % Step 3: Evaluate Fitness
    for i = 1:population_size
    cheetahs(i).fitness = evaluate_fitness(cheetahs(i).position);
    end

    % Step 4: Identify Best Solution
    best_cheetah = find_best_solution(cheetahs);

    % Step 5: Main Loop
    for iter = 1:max_iterations

    % Step 6: Update Positions
    for i = 1:population_size

    % Determine hunting strategy (exploration vs. exploitation)
    if rand() < exploration_probability % Random number for exploration
    % Exploration: Randomly move in the search space
    cheetahs(i).position = random_move(cheetahs(i).position, lower_bound, upper_bound);
    else
    % Exploitation: Move towards the best solution
    cheetahs(i).position = move_towards_best(cheetahs(i).position, best_cheetah.position);
    end

    % Step 7: Evaluate New Fitness
    cheetahs(i).fitness = evaluate_fitness(cheetahs(i).position);
    end
```

```
% Step 8: Update Best Solution
best_cheetah = find_best_solution(cheetahs);
end

% Step 9: Return Best Solution
best_solution = best_cheetah;
end

function cheetahs = initialize_population(population_size, dimension, lower_bound, upper_bound)
cheetahs = struct('position', [], 'fitness', []);
for i = 1:population_size
cheetahs(i).position = lower_bound + (upper_bound - lower_bound) * rand(1, dimension);
end

function fitness = evaluate_fitness(position)
% Define the fitness function (example: sum of squares)
fitness = sum(position.^2); % Example objective
end

function best_cheetah = find_best_solution(cheetahs)
[~, best_index] = min([cheetahs.fitness]); % Minimize fitness
best_cheetah = cheetahs(best_index);
end

function new_position = random_move(position, lower_bound, upper_bound)
% Generate a new random position within bounds
new_position = lower_bound + (upper_bound - lower_bound) * rand(size(position));

end
function new_position = move_towards_best(current_position, best_position)
% Move towards the best position (simple average strategy)
new_position = current_position + 0.1 * (best_position - current_position); % Adjust step size as needed
end
```

3. Mathematical modelling and solution for two benchmark case studies of shell-and-tube heat exchanger

The thermal design process of a Shell-and-Tube Heat Exchanger (*STHX*) involves calculating the heat transfer coefficients for both the shell and tube sides. To determine these coefficients, the correlations provided by Bell Delaware and Kern are applied, with the relevant symbols and their definitions specified in the nomenclature section. The following step-by-step approach is adopted to compute the necessary parameters:

Step 1: Calculate the heat transfer coefficients for both the tube side and the shell side using the

Reynolds number and friction factor, based on Kern's method.

Step 2: Determine the overall heat transfer coefficient using basic equations, taking into account appropriate fouling factors.

Step 3: Using the calculated overall heat transfer coefficient along with correction factors, determine the required surface area of the heat exchanger using the Log Mean Temperature Difference (*LMTD*) method.

Step 4: Evaluate the pressure drop on both the tube side and shell side of the exchanger.

Step 5: Estimate the total cost based on the surface area of the heat exchanger.

Step 6: Estimate the operational cost by factoring in the pressure drop and related energy losses.

Step 7: The total cost is derived by summing the initial installation cost and the operational cost.

3.1 Tube side heat transfer coefficient

The individual heat transfer coefficients for the Shell-and-Tube Heat Exchanger (*STHX*) are derived using the thermal design approach outlined by Kern DQ (1950). These coefficients are then used to calculate the overall heat transfer coefficients, which in turn are applied to determine the heat exchanger's surface area. The initial manufacturing cost of the *STHX* is directly linked to this surface area. Given the wide range of possible geometric configurations, it is crucial to optimize both the process and the geometric parameters. Additionally, calculating the pressure drop is important, as it impacts pump power requirements and, ultimately, operational costs. The mathematical model used to evaluate these parameters is based on established methodologies in the literature. A schematic diagram of the STHX, highlighting the primary geometric parameters is shown in Fig. 1.

The heat transfer coefficient for the tube side (h_t) is calculated based on the flow Reynolds number (*Re*), using Eqs. (3)-(4) given by Mizutani *et al*. (2003). The friction factor (*f*), which is a function of the Reynolds number and pipe roughness, is determined from existing literature, specifically utilizing the Colebrook-White equation, as given in Eqs. (1)-(2). In these equations, *d* represents the tube diameter, *L* is the tube length, *e* denotes the surface roughness of the tube material, *Pr* is the Prandtl number, and *k* is the thermal conductivity of the tube material.

$$\frac{1}{\sqrt{f}} = 1.14 - 2\,log_{10}\left(\frac{e}{d} + \frac{9.35}{Re\sqrt{f}}\right) \; for\; Re > 4000 \tag{1}$$

$$f = \frac{64}{Re} \text{ for laminar flow} \tag{2}$$

$$h_t = \frac{k_t}{d_i}\left[3.657 + \frac{0.0677\left\{R_{et}P_{rt}\left(\frac{d_i}{L}\right)\right\}^{1.33}}{1+0.1\,P_{rt}\left\{R_{et}\left(\frac{d_i}{L}\right)\right\}^{0.3}}\right] \text{ for Re < 2300} \tag{3}$$

$$h_t = \frac{k_t}{d_i}\left[\frac{(f_t/8)(R_{et}-1000)P_{rt}}{1+12.7(f_t/8)^{1/2}\left(P_{rt}^{2/3}-1\right)}\left(1+\frac{d_i}{L}\right)^{0.67}\right] \text{ for 2300 < Re < 10000} \tag{4}$$

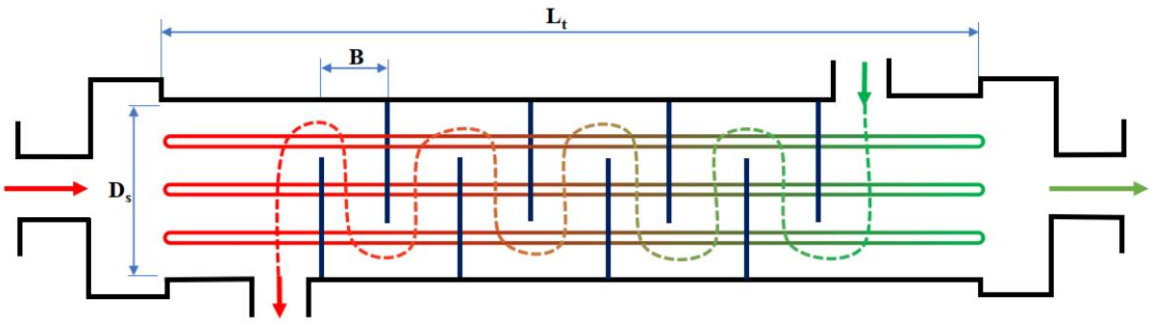

Fig. 1 Schematic diagram of the Shell-and-Tube Heat Exchanger (STHX) showing key geometric parameters

For Reynolds numbers greater than 10,000, the heat transfer coefficient is determined using Eq. (5):

$$h_t = 0.027 \frac{k_t}{d_i} \mathrm{R}_{et}^{0.8} \mathrm{P}_{rt}^{1/3} \left(\frac{\mu_t}{\mu_{tw}} \right)^{0.14} \tag{5}$$

In this context, K_t and f_t represent the thermal conductivity of the tube material and the friction factor, respectively Hewitt and Barbosa (2008)

3.2 Shell side heat transfer coefficient

Eq. (6), proposed by Kern (1950), is used to calculate the heat transfer coefficient on the shell side.

$$h_s = 0.36 \frac{k_t}{D_e} \mathrm{R}_{es}^{0.55} \mathrm{P}_{rs}^{1/3} \left(\frac{\mu_s}{\mu_{sw}} \right)^{0.14} \tag{6}$$

μ represents the dynamic viscosity of the fluid, measured at both the wall temperature and the mean fluid temperature for both the tube and shell sides. D_e denotes the equivalent diameter of the shell.

3.3 Overall heat transfer coefficient:

The overall heat transfer coefficient (U) is calculated from the individual coefficients for both sides, as outlined in Eq. (7). The associated fouling factors are incorporated based on values suggested in the literature. In the equation, R represents the fouling factor, with appropriate subscripts for the shell side and tube side.

$$U = \frac{1}{\frac{1}{h_s} + R_{fs} + \left(\frac{d_o}{d_i} \right) \left(R_{ft} + \frac{1}{h_t} \right)} \tag{7}$$

3.4 Surface area of the heat exchanger:

In standard design practice for Shell-and-Tube Heat Exchangers (*STHX*), the surface area is determined using the Log Mean Temperature Difference (*LMTD*) method. A correction factor (*F*), based on the exchanger geometry, is calculated and applied to estimate the total surface area, as shown in Eq. (8). This calculated surface area is then used to determine the pipe length, diameter, and the number of pipe turns. In this context, (*A)* represents the total surface area, while (*Q)* denotes the heat duty.

$$A = \frac{Q}{UF\Delta T_{lm}} \tag{8}$$

3.5 Frictional pressure drop on each side

Coulson and Richardson (1996) proposed Eqs. (9)-(10) for estimating the pressure drop on the tube side.

$$\Delta P_t = \frac{\rho_t {v_t}^2}{2}\left[\frac{L}{d_i} f_t + P\right] n \tag{9}$$

Kern (1950) used a value of 4 for *P*, which is also adopted in this study for comparison purposes. However, various researchers have proposed different values for *P*. In this context, ρ_t represents the fluid density, v_t is the fluid velocity within the pipe, *L* is the pipe length, and d_i is the internal diameter. The friction factor is denoted by f_t, and *n* refers to the number of tube passes.

Serna *et al*. (2007) applied Eq. (10) to estimate the pressure drop on the shell side, following the Bell-Delaware method. The relevant parameters are defined in the nomenclature table given as appendix, where *B* represents the baffle spacing and D_s denotes the shell diameter.

$$\Delta P_s = \mathrm{f}_s \left(\frac{\rho_s {v_s}^2}{2}\right)\left(\frac{L}{B}\right)\left(\frac{D_s}{D_e}\right) \tag{10}$$

3.6 Cost functions for shell-and-tube heat exchanger (STHX):

To calculate the total cost that should be minimized, it is necessary to consider the initial cost, the discounted operating cost, and the annual running cost. Caputo *et al*. (2008) presented Eq. (11) to determine the overall cost of the heat exchanger, which accounts for both the initial investment and the discounted ongoing operating costs.

$$C_T = C_I + C_{doc} \tag{11}$$

In this context, C_{doc} refers to the discounted operating cost, and C_I represents the initial capital investment, together constituting the total cost C_T. Furthermore, Taal *et al*. (2003) introduced Eq. (12) to estimate the initial cost of the heat exchanger.

$$C_I = a_1 + a_2 A^{a_3} \tag{12}$$

Here, a_1, a_2 and a_3 are numerical constants whose values are taken from Taal *et al*. (2003), and *A* represents the surface area. The pumping power affects the discounted operating cost, which is

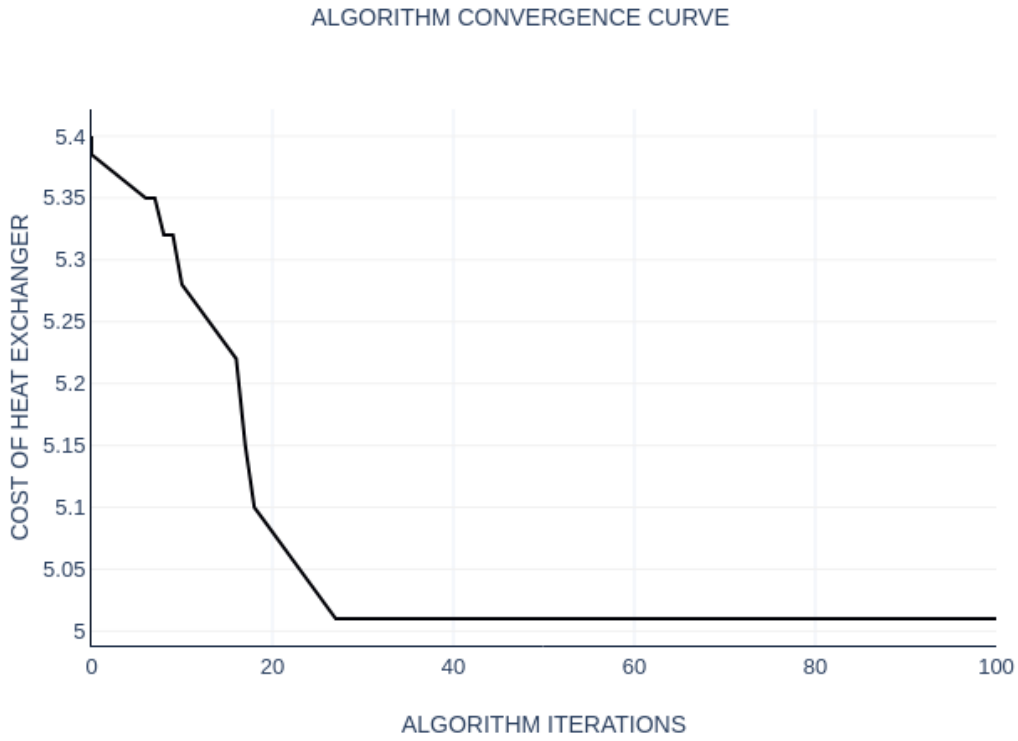

Fig. 2 Convergence curve of the algorithm for the methanol-brackish water heat exchanger in case study 1

given by Eq. (13), as proposed by Caputo *et al*. (2008).

$$C_{doc} = \sum_{j=1}^{n_y} \frac{c_o}{(1+i)^j} \tag{13}$$

In this context, n_y represents the number of years the equipment operates, and i denotes the annual inflation rate, set at 10%. The operating cost is expressed by Eq. (14).

$$C_o = P_1 C_e H \tag{14}$$

Here, P_1 represents the corresponding pumping power, as defined in Eq. (15). C_e is the electricity cost, and H denotes the annual operating hours of the heat exchanger.

$$P_1 = \frac{1}{\eta}\left(\frac{m_t}{\rho_t}\Delta P_t + \frac{m_s}{\rho_s}\Delta P_s\right) \tag{15}$$

The corresponding pressure drop is determined using Eqs. (9)-(10).

3.7 Solution of benchmark design problem

The design optimization case studies for the shell and tube heat exchanger (*STHX*) are based on the work of Kern (1950). These case studies have been widely analysed by various researchers, providing opportunities for comparison and validation of the results.

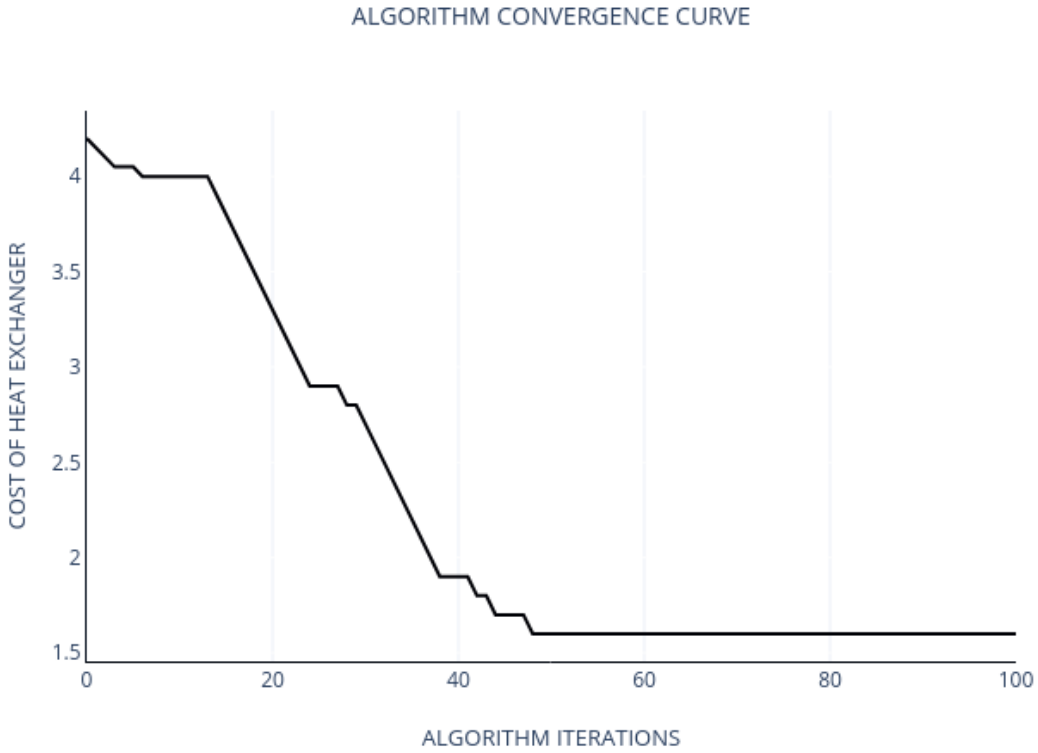

Fig. 3 Convergence curve of the algorithm for the kerosene-crude oil heat exchanger in case study 2

The first case study involves a methanol-brackish water *STHX* with a heat duty of 4.34 MW, featuring one shell and two tube passes. The results obtained using the Cheetah Optimizer (*CO*) are compared with those from other optimization methods, including Particle Swarm Optimization (*PSO*), α-EHO, Adaptive SOS, and GSA calculated by Patel and Rao (2010) and Makadia (2021).

The second case study focuses on a kerosene-crude oil STHX with a heat duty of 1.44 MW, configured in a 1-4 pass arrangement. Fig. 2 and Table 1 illustrate the details for case study 1, while Fig. 3 and Table 2 correspond to case study 2.

The design variables—shell diameter (D_s), tube outer diameter (d_o), and baffle spacing (B)—are constrained based on guidelines provided by the Tubular Exchanger Manufacturers Association (*TEMA*). The convergence criteria for the optimization process are set in accordance with these geometric limits, with a maximum of 100 iterations. However, convergence was typically achieved within 25 iterations for benchmark problem 1 and within 50 iterations for benchmark problem 2, as shown in Figs. 2-3.

The geometric constraints are as follows:

- $0.1 \leq D_s \leq 1.5$
- $0.015 \leq d_o \leq 0.051$
- $0.05 \leq B \leq 0.5$

All dimensions are provided in meters (m).

The algorithm convergence curve for the Methanol-Brackish Water heat exchanger and kerosene crude oil heat exchanger (Case Study 1 and 2 respectively) illustrates the progress of the

Table 1 Parameter and cost value for Methanol Brackish water heat exchanger – case study 1

Parameter	PSO	Adaptive SOS	α- EHO	GSA	Cheetah Optimizer (Current work)
L (m)	3.115	2.204	2.855	2.783	2.559
d_o (m)	0.015	0.014	0.015	0.015	0.015
B (m)	0.424	0.48	0.395	0.486	0.483
D_s (m)	0.81	0.78	0.77	0.842	0.79
N_t	1658	2960	1698	1806	1789
v_t (m/s)	0.67	0.69	0.66	0.678	0.66
Re_t	10503	9677	10156	10118	9988
Pr_t	5.7	5.7	5.7	5.7	5.7
h_t (w/m^2K)	3721	3941	3653	4029	3648
f_t	0.0311	0.03	0.03	0.031	0.03
d_e (m)	0.0107	0.01	0.01	0.0107	0.01
v_s (m/s)	0.53	0.49	0.69	0.453	0.48
Re_s	12678	8639	12813	10662	11789
Pr_s	5.1	5.1	5.1	5.1	5.1
h_s (W/m^2K)	1950.8	2219.2	2142	2060	2200
f_s	0.349	0.34	0.34	0.358	0.35
ΔP_s (Pa)	20551	15774	22456	12458	21956
U (W/m^2K)	713.9	784	758	732.6	766
A (m^2)	243.2	236.1	216	236.9	245
C_I (€)	46453	45048	40556	45439	45400
C_o (€/yr)	1038.7	1001	1076	813.2	1066
C_{doc}(€)	6778.2	6258	6645	4673	5998
C_{total} (€)	53231	51306	47201	50112	51398
ΔP_t (Pa)	4171	5854	4166	4501	5100

optimization algorithm in minimizing the design objective (such as cost or energy efficiency) over the course of iterations.

In the context of Case Study 1 and 2, this convergence curve would typically show how the algorithm approaches a solution as the number of iterations increases. The key features to include in this curve would be:

X-axis (Iterations): This would represent the number of iterations performed by the optimization algorithm, starting from 1 and increasing until the maximum iteration limit or until convergence is achieved.

Y-axis (Objective function value): This would represent the value of the objective function (such as the total cost, energy consumption, or heat transfer efficiency) being optimized. The value should decrease or stabilize as the optimization algorithm approaches the optimal solution.

Initially, the objective function value will vary significantly as the algorithm explores various design variables. As the algorithm progresses, the curve should show a general downward trend, indicating that the optimization is finding better solutions. The curve will eventually plateau or

Table 2 Parameter and cost value for kerosene crude oil heat exchanger – case study 2

Parameter	PSO	Adaptive SOS	α- EHO	GSA	Cheetah Optimizer (Current work)
L *(m)*	1.56	1.39	1.48	1.317	1.3
d_o *(m)*	0.015	0.012	0.013	0.015	0.015
B *(m)*	0.11	0.13	0.11	0.11	0.11
D_s *(m)*	0.63	0.46	0.51	0.62	0.6
N_t	646	702	681	718	678
v_t *(m/s)*	0.93	1.25	1.01	0.75	1.1
Re_t	3283	3091	3217	3102	3201
Pr_t	55.2	55.1	55.2	55.2	55.1
h_t *(w/m²K)*	1205	1414	1316	1488	1313
f_t	0.044	0.06	0.051	0.046	0.05
d_e *(m)*	0.0149	0.014	0.014	0.0148	0.014
v_s *(m/s)*	0.495	0.6	0.515	0.476	0.49
Re_s	15844	14947	15111	15004	15900
Pr_s	7.5	7.5	7.5	7.5	7.5
h_s *(W/m²K)*	1288	1537	1482	1512	1480
f_s	0.337	0.336	0.336	0.34	0.336
ΔP_s *(Pa)*	21745	23145	22054	17962	20800
U *(W/m²K)*	409.3	503	461	348	419
A *(m²)*	47.5	43.2	46	54.98	45.4
C_I *(€)*	16707	15987	16112	17639	16888
C_o *(€/yr)*	523.3	611	571	290.1	435
C_{doc}*(€)*	3215.6	3487	3396	1642	3110
C_{total} *(€)*	19922	19474	19508	19281	19998
ΔP_t *(Pa)*	16926	18012	17450	8449	17112

show minimal fluctuations, which suggests convergence towards an optimal or near-optimal solution.

Fig. 2 depicts the convergence curve for Case Study 1. At the start of the first iteration, the total cost is approximately 5.4K. As the optimization progresses, the cost steadily decreases, reaching just above 5.0K by the 25th iteration, at which point convergence is achieved. After this point, the cost remains unchanged, indicating that the algorithm converges early in the process.

Table 1 provides the geometric and cost parameters derived from applying the Cheetah Optimizer to the design problem. The results show a 3 % reduction in the total cost compared to the Particle Swarm Optimization (*PSO*) method. This cost reduction is accompanied by a 2 % decrease in the shell diameter and a significant 17 % reduction in the tube length. There is no major change in the tube's outer diameter, but a small 2 % decrease in the tube side heat transfer coefficient is observed. Additionally, the Reynolds number for the shell-side fluid flow decreases, while the heat transfer coefficient for the shell side increases by 11.3 %, which is attributed to localized disturbances within the fluid flow. The overall surface area of the shell-and-tube heat

exchanger (*STHX*) increases by 0.7% compared to the PSO results, driven by the higher overall heat transfer coefficient. Operating costs have slightly risen due to the higher shell-side pressure drop. The highest heat transfer coefficient among all methods is achieved with the Adaptive SOS technique, at 784 W/m²K, which is approximately 9 % higher than the values obtained using PSO and the Cheetah Optimizer. The results obtained thus shows that the Cheetah Optimizer can be effectively utilized for real world design engineering and optimization problems. However, it can be applied on other applications to prove its efficacy as it did not outperform Adaptive SOS and α-EHO optimization.

Fig. 3 presents the convergence curve for Case Study 2. As shown, the cost decreases significantly from 4.5K to 1.5K between the first and 45th iterations. The algorithm achieves convergence at the 45th iteration, as indicated in the Fig.3. Table 2 lists the geometric and cost parameters for Case Study 2, based on the results from applying the Cheetah algorithm. Unlike Case Study 1, no significant reduction in the overall cost of the STHX is observed with the Cheetah Optimizer compared to the PSO method. However, the shell diameter is reduced by 4 %, and the tube length decreases by 16 %. The Cheetah Optimizer also results in a 4 % reduction in the overall surface area. Additionally, the overall heat transfer coefficient is 2 % higher than that obtained with the PSO method. These results are further compared with those obtained using the α-EHO technique for the same problem. It is observed that for this particular case study the Cheetah Optimizer was not able to outperform any other optimization technique. Henceforth, it is required that more exploration of this method needs to be performed so as to prove its efficacy in real world design engineering problems.

The findings demonstrate that the Cheetah algorithm offers significant benefits for *STHX* design challenges. Moreover, results also indicate a highly nonlinear nature of the design problem which indicates results departing from fundamentals. This demands further work which could validate these results further by employing other nature-inspired metaheuristics, and the proposed approach could be applied to real-world engineering design problems.

4. Mathematical modelling and solution of benchmark case study of Plate fin heat exchanger

4.1 Thermal modelling of PFHE

This study focuses on the optimization of a cross-flow plate fin heat exchanger *(PFHE)* with an offset strip fin design. Fig. 4 shows the schematic diagram of the PFHE geometry being analysed. For a cross-flow heat exchanger where the two fluids do not mix, the effectiveness *(ϵ)* is defined by Incropera *et al*. (1996), as described in Eq. (16).

$$\varepsilon = 1 - exp\left[\left(\frac{1}{C_r}\right) NTU^{0.23}[exp(-C_r NTU^{0.78}) - 1]\right] \tag{16}$$

The heat capacity ratio (C_r) and Number of transfer units (*NTU*) are given as Eq. (17).

$$\frac{1}{NTU} = \frac{C_{\min}}{UA} = C_{\min}\left[\frac{1}{(hA)_h} + \frac{1}{(hA)_c}\right] \tag{17}$$

The subscripts *h* and *c* refer to the hot-side fluid and cold-side fluid, respectively. The free flow area (A_{ff}) for the plate fin heat exchanger geometry is given by Eqs. (18)-(19).

$$A_{ff,h} = (H_h - t_h)(1 - n_h t_h) L_c N_h \tag{18}$$

$$A_{ff,c} = (H_c - t_c)(1 - n_c t_c) L_h N_c \tag{19}$$

Here, L_c and L_h represent the cold-side and hot-side flow lengths, respectively, while N_h and N_c denote the number of layers on the hot and cold sides. The heat transfer areas (A) for both sides are calculated using Eqs. (20)-(21).

$$A_h = L_h L_c N_h [1 + 2n_h (H_h - t_h)] \tag{20}$$

$$A_c = L_h L_c N_c [1 + 2n_c (H_c - t_c)] \tag{21}$$

Henceforth Eq. (22) gives the total heat transfer area.

$$A = A_h + A_c = L_h L_c \left[N_h \left(1 + 2n_h (H_h - t_h)\right) + N_c \left(1 + 2n_c (H_c - t_c)\right) \right] \tag{22}$$

The Colburn factor (j), Fanning factor (f), and heat transfer coefficient for the offset strip fin are provided by Manglik and Bergles (1995), as expressed in Eq. (23).

$$j = 0.6522 (\mathrm{Re})^{-0.5403} (\alpha)^{-0.1541} (\delta)^{0.1499} (\gamma)^{-0.0678} \left[1 + 5.269 \times 10^{-5} (\mathrm{Re})^{1.34} (\alpha)^{0.504} (\delta)^{0.456} (\gamma)^{-1.055} \right]^{0.1}$$
$$f = 9.6243 (Re()^{-0.7422} (\alpha)^{-0.1856} (\delta)^{0.3053} (\gamma)^{-0.2659}) \tag{23}$$

$$h = jGC_p (\mathrm{Pr})^{-0.667} \tag{24}$$

where Re, α, δ, γ and f_s are dimensionless parameters and given by Eq. (25),

$$Re = \frac{G d_h}{\mu},\ \alpha = \frac{fs}{H - t},\ \delta = \frac{t}{l_f},\ \gamma = \frac{t}{fs},\ fs = \left(\frac{1}{n} - t\right) \tag{25}$$

The aforementioned equations for the Colburn factor *(j)* and Fanning factor *(f)* are applicable for

$$120 < Re < 10^4,\ 0.134 < \alpha < 0.997,\ 0.012 < \delta < 0.048,\ 0.041 < \gamma < 0.121$$

For the specified fin geometry, the hydraulic diameter *(d_h)* is calculated using Eq. (26).

$$d_h = \frac{4 fs l_f (H - t)}{2\left(fs l_f + (H - t) l_f + (H - t) t + t fs\right)} \tag{26}$$

The frictional pressure drop for the two fluid streams is provided by Shah and Sekulic (2003) in Eqs. (27)-(28).

$$\Delta P_h = \frac{2 f_h L_h {G_h}^2}{\rho_h d_{h,h}} \tag{27}$$

$$\Delta P_c = \frac{2 f_c L_c {G_c}^2}{\rho_c d_{h,c}} \tag{28}$$

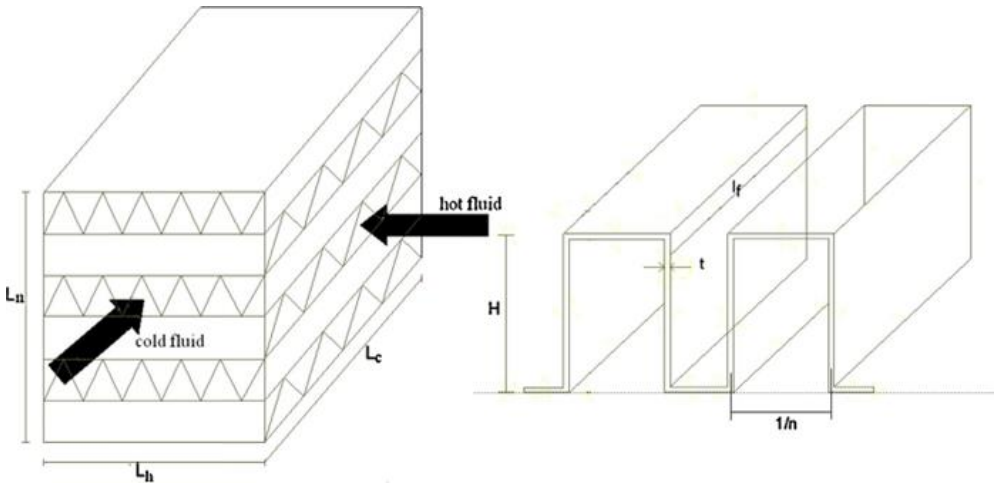

Fig. 3 Geometry and layout of plate fin heat exchanger

Table 3 Parameters for cost evaluation of plate fin heat exchanger

Parameter	Magnitude
Electricity cost ($), in dollars per megawatt-hour ($/MWh)	20
Non-linear exponent (n_1)	0.6
Interest rate (ROI), expressed as a percentage	0.1
Operating hours (τ), in hours (h)	5000
Cost per unit area (CA), in dollars per square meter ($/m²)	90
Depreciation period (z_1), in years.	10
Efficiency of compressor (η)	0.6

4.2 Objective function for PFHE

The total annual cost (TAC) of a plate fin heat exchanger ($PFHE$) includes two main components: the initial cost (C_{in}) and the operating cost (C_{op}). To maintain consistency in comparisons, both costs are calculated using the same cost function from the previous work of Yousefi *et al*. (2012). The initial cost of the heat exchanger is estimated using the correlation provided in Eq. (29).

$$C_{in} = A_{cf} C_A A^{n_1} \tag{29}$$

Here, C_A represents the cost per unit surface area, and n_1 is the exponent that describes the nonlinear increase in cost with respect to the surface area. A_{cf} is the annual coefficient factor, which is calculated using Eq. (30).

$$A_{cf} = \frac{roi}{1 - (1 + roi)^{-z_1}} \tag{30}$$

Here, roi represents the interest rate, and z_1 denotes the depreciation period. The operating cost is determined by the pumping power required to circulate the hot and cold fluids through the exchanger, and it is calculated using Eq. (31).

Table 4 Thermal and fluid operating parameters for plate fin heat exchanger

Parameters	Hot side	Cold side
Viscosity (μ), in newton-seconds per square meter (N·s/m²)	4.01E−05	3.36E−05
Inlet temperature (T), in degrees Celsius (°C)	900	200
Mass flow rate (m), in kilograms per second (kg/s)	1.66	2
Density (ρ), in kilograms per cubic meter (kg/m³)	0.6296	0.9638
Specific heat (Cp), in joules per kilogram per Kelvin (J/kg·K)	1122	1073
Prandtl number (*Pr*)	0.731	0.694

Table 5 Parameter and cost value for plate fin heat exchanger

Design Variable	ICA Approach	TLBO Approach	Cheetah Optimizer approach (This work)
Hot side pressure drop (ΔPh), kPa	0.28	0.304	0.3
Hot side flow length (L_h), m	0.83	0.8353	0.83
Number of hot side layer (N_h)	73	71	71
Cold side pressure drop (ΔPc), kPa	0.31	0.33	0.33
Cold side flow length (L_c), m	1	1	1
No flow length (L_n), m	1.5	1.5	1.4
Lance length of fin (l_f), mm	10	8.296	9.1
Fin frequency (n), m−1	228.2	205.2	210
Fin thickness (t), mm	0.2	0.1921	0.191
Fin height (H), mm	9.7	9.986	9.9
Function evaluations	12,000	8000	2000
Computational time (s)	3.55	2.63	2.89
Initial cost ($)	713.2	679.91	670.4
Operating cost ($)	228.8	247.72	244.2
Total cost ($)	942	927.63	914.6

$$C_{op} = \left[\zeta\tau\frac{\Delta Pm}{\eta\rho}\right]_h + \left[\zeta\tau\frac{\Delta Pm}{\eta\rho}\right]_c \tag{31}$$

All the parameters necessary for cost evaluations in the current study are provided in Table 3.

A gas-to-air single-pass cross-flow heat exchanger with a heat duty of 1069.8 kW is designed and optimized to minimize the total annual cost. The exchanger's maximum dimensions are constrained to 1 m × 1 m × 1.5 m. Both the hot and cold sides of the heat exchanger feature offset strip fin surfaces with identical specifications. The material used for construction is aluminium, with a density of 2700 kg/m³. The allowable pressure drops are 9.50 kPa for the hot side and 8.00 kPa for the cold side. Table 4 outlines the operating conditions for the Plate Fin Heat Exchanger *(PFHE)*.

The fluid inlet temperatures and flow rates are provided as design specifications. Seven design variables are considered for the optimization process: hot side flow length *(L_h)*, cold side flow length *(L_c)*, fin height *(H)*, fin thickness *(t)*, fin frequency *(n)*, fin lance length *(l_f)*, and the number of hot side layers *(N_h)*.

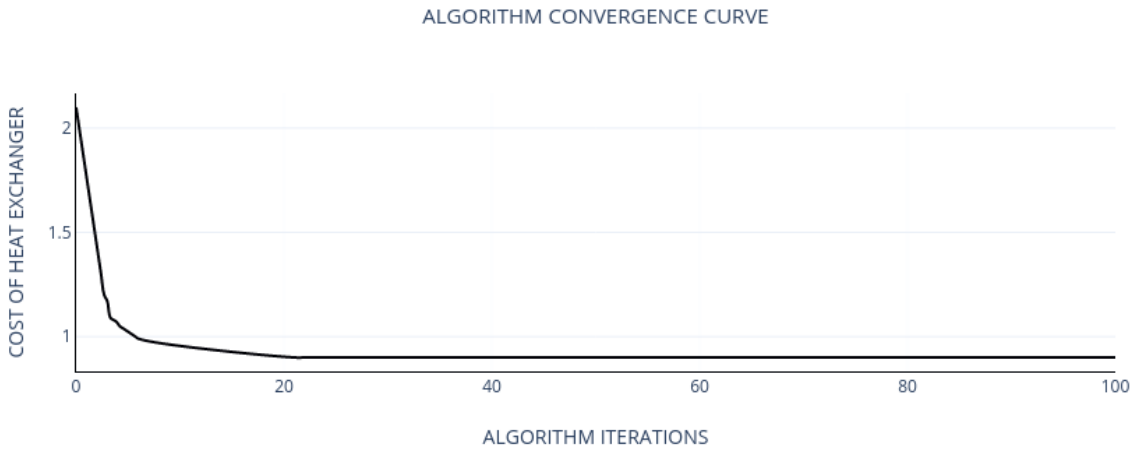

Fig. 4 Algorithm convergence curve for plate fin heat exchanger

In this study, a proposed method is applied to solve the single-objective constrained minimization problem. The goal is to minimize the total annual cost of the heat exchanger. To address constraint violations during the optimization, a static penalty term is incorporated into the objective function. This function is subject to seven inequality constraints, determined by the upper and lower bounds of the design variables.

$0.1 \leq L_h \leq 1$, $0.1 \leq L_c \leq 1$, $0.002 \leq H \leq 0.01$, $100 \leq n \leq 1000$, $0.0001 \leq t \leq 0.0002$, $0.001 \leq l_f \leq 0.01$, $1 \leq N_h \leq 200$, $\Delta P_h \leq 9.50\ kPa$, $\Delta P_c \leq 8\ kPa$.

Table 5 and Fig. 4 present the results and the algorithm's convergence curve for the plate fin heat exchanger cost optimization case study. As illustrated in Fig. 4, the initial cost of the heat exchanger starts just above 2K and decreases to 0.9K within 2000 iterations. Compared to the Imperialist Competitive Algorithm *(ICA)*, there is a notable improvement of 3% in the overall cost. When comparing the Cheetah Optimizer results to those of the ICA, the fin height *(H)* shows a slight increase. Additionally, the frequency of fin placement has decreased by 7% relative to the ICA. While the computational time for the Cheetah Optimizer is greater than that of the TLBO method, it is still less than that of the ICA.

These results suggest that the Cheetah Optimizer algorithm performs well in comparison to both ICA and TLBO methods, demonstrating its potential for application in real-world design challenges involving plate fin heat exchangers.

5. Conclusions

• Effective Application: The Cheetah Optimizer shows promise in optimizing design problems for shell and tube heat exchangers and plate fin heat exchangers.

• Performance Validation: Results obtained using the Cheetah Optimizer were validated against various established metaheuristic methods, ensuring the robustness of the findings.

• Cost Reduction: For the shell and tube heat exchanger, the Cheetah Optimizer achieved a notable 3% reduction in overall costs compared to Particle Swarm Optimization *(PSO)*.

• Comparative Performance: Although the Cheetah algorithm did not outperform α-EHO and Gravitational Search Algorithm *(GSA)* in case study 1, it outperformed GSA and α-EHO in case

study 2.

• Plate Fin Heat Exchanger Results: The Cheetah Optimizer demonstrated superior performance compared to both the Imperialist Competitive Algorithm and Teaching Learning-Based Optimization in the plate fin heat exchanger optimization.

Henceforth, The Cheetah Optimizer is a viable alternative for optimizing heat exchanger designs, offering competitive results against established algorithms in certain scenarios.

References

Akbari, M.A., Zare, M., Azizipanah-Abarghooee, R., Mirjalili, S. and Deriche, M. (2022), "The cheetah optimizer: A nature-inspired metaheuristic algorithm for large-scale optimization problems", *Sci. Rep.*, **12**(1), 10953. https://doi.org/10.1038/s41598-022-14338-z.

Babu, B.V. and Munawar A. Shaik. (2007), "Differential Evolution Strategies for Optimal Design of Shell-and-Tube Heat Exchangers", *Chem. Eng. Sci.*, **62**, 3720-3739. https://doi.org/10.1016/j.ces.2007.03.039.

Bahiraei, M., Foong, L.K., Hosseini, S. and Mazaheri, N. (2021), "Neural network combined with nature-inspired algorithms to estimate overall heat transfer coefficient of a ribbed triple-tube heat exchanger operating with a hybrid nanofluid", *Measurement*, **174**, 108967. https://doi.org/10.1016/j.measurement.2021.108967.

Caputo, A.C., Pelagagge, P.M. and Salini, P. (2008), "Heat exchanger design based on economic optimization", *Appl. Therm. Eng.*, **28**(10), 1151-1159. https://doi.org/10.1016/j.applthermaleng.2007.08.010.

Coulson, J.M. and Richardson, J.F. (1996), *Coulson & Richardson's Chemical Engineering*, Butterworth-Heinemann, Oxford, U.K.

Fesanghary, M., Damangir, E. and Soleimani, I. (2009), "Design optimization of shell and tube heat exchangers using global sensitivity analysis and harmony search algorithm", *Appl. Therm. Eng.*, **29**(5-6), 1026-1031. https://doi.org/10.1016/j.applthermaleng.2008.05.018.

Ghanei, A., Assareh, E., Biglari, M., Ghanbarzadeh, A. and Noghrehabadi, A.R. (2014), "Thermal-economic multi-objective optimization of shell and tube heat exchanger using particle swarm optimization (PSO)", *Heat Mass Transf.*, **50**, 1375-1384. https://doi.org/10.1016/j.pnucene.2024.105416.

Hajabdollahi, M., Shafiey Dehaj, M. and Hajabdollahi, H. (2021), "Investigation of optimization algorithms and their operating parameters in different types of heat exchangers", *Energy Equip. Syst.*, **9**(4), 351-370. https://doi.org/10.22059/ees.2021.248626.

Hewitt, G.F. and Barbosa, J. (2008), *Heat exchanger Design Handbook* (Vol. 98), Begell House, New York, U.S.A.

Incropera, F.P., DeWitt, D.P., Bergman, T.L. and Lavine, A.S. (1996), *Fundamentals of Heat and Mass Transfer* (Vol. 6, p. 116), Wiley, New York, U.S.A.

Jafari-Asl, J., Montaño, O.D.L., Mirjalili, S. and Faes, M.G. (2024), "A meta-heuristic approach for reliability-based design optimization of shell-and-tube heat exchangers", *Appl. Therm. Eng.*, **248**, 123161. https://doi.org/10.1016/j.applthermaleng.2024.123161.

Kaveh, A. and Farhoudi, N. (2016), "Dolphin echolocation optimization: continuous search space", *Adv. Comput. Des.*, **1**(2), 175-194. https://doi.org/10.12989/acd.2016.1.2.175.

Kaveh, A. and Rezaei, M. (2016), "Topology and geometry optimization of different types of domes using ECBO", *Adv. Comput. Des*, **1**(1), 1-25. https://doi.org/10.12989/acd.2016.1.1.001.

Kern, D.Q. (1950). *Process Heat Transfer* (Vol. 871). McGraw-Hill. United States.

Lara-Montaño, O.D., Gómez-Castro, F.I., Gutiérrez-Antonio, C. and Dragoi, E.N. (2025), "Success-Based Optimization Algorithm (SBOA): Development and enhancement of a metaheuristic optimizer", *Comput. Chem. Eng.*, **194**, 108987. https://doi.org/10.1016/j.compchemeng.2024.108987.

Makadia, J. (2021), "Adaptive symbiotic organisms search technique for cost optimization of shell and tube heat exchanger", *J. Therm. Eng.*, **10**(4), 857-867. https://doi.org/10.14744/thermal.0000837.

Manglik, R.M. and Bergles, A.E. (1995), "Heat transfer and pressure drop correlations for the rectangular offset strip fin compact heat exchanger", *Experim. Therm. Fl. Sci.*, **10**(2), 171-180. https://doi.org/10.1016/0894-1777(94)00096-Q.

Mekki, B.S., Langer, J. and Lynch, S. (2021), "Genetic algorithm based topology optimization of heat exchanger fins used in aerospace applications", *Int. J. Heat Mass Transf.*, **170**, 121002. https://doi.org/10.1016/j.ijheatmasstransfer.2021.121002.

Mizutani, F.T., Pessoa, F.L., Queiroz, E.M., Hauan, S. and Grossmann, I.E. (2003), "Mathematical programming model for heat-exchanger network synthesis including detailed heat-exchanger designs: 1. Shell-and-tube heat-exchanger design", *Ind. Eng. Chem. Res.*, **42**(17), 4009-4018. https://doi.org/10.1021/ie020964u.

Mohapatra, S., Das, D.K. and Singh, A.K. (2024), "An optimal plate-fin heat exchanger design using opposition-based Orthogonal Learning Kho-Kho Optimization algorithm", *Prog. Nucl. Energy*, **177**, 105416. https://doi.org/10.1016/j.pnucene.2024.105416.

Patel, V.K. and Rao, R.V. (2010), "Design optimization of shell-and-tube heat exchanger using particle swarm optimization technique", *Appl. Therm. Eng.*, **30**(11-12), 1417-1425. https://doi.org/10.1016/j.applthermaleng.2010.03.001.

Saldanha, W.H., Arrieta, F.R.P. and Soares, G.L. (2021), "State-of-the-art of research on optimization of shell and tube heat exchangers by methods of evolutionary computation", *Arch. Comput. Meth. Eng.*, **28**, 2761-2783. https://doi:10.1007/s11831-020-09476-4.

Serna-González, M., Ponce-Ortega, J.M., Castro-Montoya, A.J. and Jiménez-Gutiérrez, A. (2007), "Feasible design space for shell-and-tube heat exchangers using the Bell−Delaware method", *Ind. Eng. Chem. Res.*, **46**(1), 143-155. https://doi.org/10.1021/ie051371x.

Shah, R.K. and Sekulic, D.P. (2003), *Fundamentals of Heat Exchanger Design*, John Wiley & Sons, Hoboken, New Jersey, U.S.A.

Silva, A.P., Ravagnani, M.A., Biscaia, E.C. and Caballero, J.A. (2010), "Optimal heat exchanger network synthesis using particle swarm optimization", *Optim. Eng.*, **11**, 459-470. https://doi.org/10.1007/s11081-009-9089-z.

Taal, M., Bulatov, I., Klemeš, J. and Stehlík, P. (2003), "Cost estimation and energy price forecasts for economic evaluation of retrofit projects", *Appl. Therm. Eng.*, **23**(14), 1819-1835. https://doi.org/10.1016/S1359-4311(03)00136-4.

Thuy, N.T.P., Pendyala, R., Rahmanian, N. and Marneni, N. (2014), "Heat exchanger network optimization by differential evolution method", *Appl. Mech. Mater.*, **564**, 292-297. https://doi.org/10.4028/www.scientific.net/AMM.564.292.

Xie, G., Wang, Q. and Sunden, B. (2008), "Application of a genetic algorithm for thermal design of fin-and-tube heat exchangers", *Heat Transf. Eng.*, **29**(7), 597-607. https://doi.org/10.1080/01457630801922337.

Yousefi, M., Darus, A.N. and Mohammadi, H. (2012), "An imperialist competitive algorithm for optimal design of plate-fin heat exchangers", *Int. J. Heat Mass Transf.*, **55**(11-12), 3178-3185. https://doi.org/10.1016/j.ijheatmasstransfer.2012.02.041.

Yousefi, M., Darus, A.N., Yousefi, M. and Hooshyar, D. (2015), "Multi-stage thermal-economical optimization of compact heat exchangers: A new evolutionary-based design approach for real-world problems", *Appl. Therm. Eng.*, **83**, 71-80. https://doi.org/10.1016/j.applthermaleng.2015.03.011.

CC

Nomenclature

Nomenclature for shell and tube heat exchanger:

A	Surface area (m^2)
ΔP	Friction pressure loss (Pa)
h	Heat transfer coefficient (W/m^2K)
R_e	Reynolds No.
P_r	Prandlt No.
U	Overall heat transfer coefficient (W/m^2K)
Q	Heat transfer rate (MW)
ρ	Fluid density (kg/m^3)
C_I	Initial capital investment (€)
C_{doc}	Discounted operating cost (€)
C_o	Yearly running cost (€/yr)
C_e	Energy price (€/KWh)
CT	Total cost
f	Friction factor
μ	Viscosity at mean fluid and corresponding wall temperature (Pa s)
R	Fouling factor (m^2 K/W)
F	Geometry based correction factor for LMTD
ΔT_{lm}	Logarithmic mean temperature difference
v	Fluid velocity (m/s)
n	No. of tube passes
D_e	Equivalent shell diameter (m)
d	diameter of tube (m)
e	Pipe roughness (m)

k_t	Tube material thermal conductivity (W/mK)
L	Length of tube (m)
m	flow rate (kg/s)
D_s	Shell diameter (m)
η	Pump Efficiency
n_y	Equipment life in years
H	Working hours
B	Baffle spacing (m)
P_l	Pumping Power (W)
PSO	Particle Swarm Optimization
α-EHO	Alpha tuning elephant herding optimization
STHX	Shell and tube heat exchanger

Nomenclature for plate fin heat exchanger:

f	Fanning friction factor
h	Convective heat transfer coefficient (W/m^{2}K)
Pr	Prandtl number
j	Colburn factor
A	Heat exchanger surface area (m^2)
C_{op}	Operating cost ($)
C_{in}	Initial cost ($)
n	Fin frequency (m^{-1})
H	Height of fin (m)
NTU	Number of transfer units
L	Heat exchanger length (m)
A_{ff}	Free flow area (m^2)
A_{cf}	Annual coefficient factor

G	Mass flux velocity (kg/m^{2}S)
n_1	Exponent of non linear increase with area increase
ΔP	Pressure drop (KPa)
U	Overall heat transfer coefficient
Re	Reynolds Number
N_h	Number of hot side layer
C_A	Cost per unit area ($/m^2)
C_p	Specific heat (J/kgK)
C_r	Heat capacity ratio (c_{min}/C_{max})
C	Heat capacity rate (W/k)
l_f	Lance length of the fin (m)
z_1	Depreciation time
F_s	Fin spacing (m)
t	Fin thickness (m)
d_h	Hydraulic diameter (m)
m	Mass flow rate (kg/s)
T	Temperature (^{o}C)
roi	Rate of interest
TAC	Total annual cost

Roman symbols

ρ	Density (Kg/m^3)
$\$$	Electricity price ($/MWhr)
τ	Hour of operation
μ	Viscosity (Ns/m^2)
ε	Effectiveness
η	Compressor efficiency

subscripts

c	Cold
h	Hot
min	Minimum
max	Maximum